STUDIECENTRUM VOOR KERNENERGIE
CENTRE D'ÉTUDE DE L'ÉNERGIE NUCLÉAIRE

OPEN REPORT
SCK•CEN-BLG-1016

The Use of Single-Specimen Techniques for Measuring Upper Shelf Toughness Properties under Impact Loading Rates

Convention TRACTEBEL/SCK•CEN 2005
Task 1.1.5

E. Lucon

September, 2005

SCK•CEN
Boeretang 200
2400 Mol
Belgium

OPEN REPORT OF THE BELGIAN NUCLEAR RESEARCH CENTRE
SCK•CEN-BLG-1016

The Use of Single-Specimen Techniques for Measuring Upper Shelf Toughness Properties under Impact Loading Rates

Convention TRACTEBEL/SCK•CEN 2005
Task 1.1.5

E. Lucon

September, 2005
Status: Unclassified
ISSN 1379-2407

SCK•CEN
Boeretang 200
2400 Mol
Belgium

Name	Institute	Number
E. Lucon	SCK•CEN, RMO	1
J.-L. Puzzolante	SCK•CEN, RMO	1
J. Schuurmans	SCK•CEN, RMO	1
M. Scibetta	SCK•CEN, RMO	1
E. van Walle	SCK•CEN, RMO	1
	Secretariaat RMO	3
R. Gérard	Tractebel Engineering	3

Belgian Nuclear Research Centre
Boeretang 200
2400 Mol
Belgium

Phone +32 14 33 21 11
Fax +32 14 31 50 21

http://www.sckcen.be

Contact:
Knowledge Centre
library@sckcen.be

Table of contents

Abstract

The multiple-specimen method (low-blow or stop-block tests) is the conventional approach for measuring the upper shelf fracture toughness of metallic materials under impact loading rates, typically fatigue precracked Charpy specimens tested on an instrumented pendulum machine. The method is fairly simple but requires a relatively large number of specimens.

Nowadays, several single-specimen methods are available, which are purely based on the analysis of the instrumented force/displacement trace; they don't need any dedicated instrumentation for the measurement of crack extension during the test. Three of these techniques have been applied in this work to low-blow tests performed at different temperatures on two significantly different RPV steels (20MnMoNi55 and JSPS): the Normalization Data Reduction (NDR) technique, Schindler's Analytical 3-Parameter Approach and Chaouadi's method.

Analyses have been performed after applying a double fitting approach to the raw test data, which allows selecting a limited set of force/displacement data which are representative of the whole instrumented trace.

Results show that all three methods provide acceptable accuracy in terms of both ductile crack initiation and resistance to crack propagation (tearing modulus). However, for this type of analysis we recommend the use of the more widely accepted NDR technique, which is described in detail in the ASTM E1820-01 standard (although the limitations on data smoothness presently enforced in the standard seem incompatible with the oscillations of a typical dynamic PCCv curve).

Keywords

Multiple-specimen method, low-blow tests, upper shelf toughness, precracked Charpy specimens, instrumented impact tests, single-specimen methods, Normalization Data Reduction, Schindler's key curve, Chaouadi's approach, tearing modulus.

1 Introduction

The knowledge of dynamic mechanical properties is useful in all circumstances where strain rate sensitivity of a metallic material is an issue, and whenever the actual loading conditions for a structure (either in normal operation or under accidental circumstances) are different from static. Furthermore, in some investigations increasing the strain (loading) rate in a mechanical test is used to simulate other embrittling mechanisms, such as heat treatments or exposure to neutron irradiation.

The instrumentation of the pendulum striker in a Charpy test allows measuring dynamic fracture toughness on fatigue precracked specimens and consequently use the results for structural integrity assessments. For a precracked Charpy (PCCv) specimen with a/W ≈ 0.5 tested at 1.5 m/s, the corresponding loading rate, expressed in terms of increase of stress intensity factor $\dot{K}$, is of the order of 10^5 MPa√m/s.

As far as fracture toughness test standards are concerned, most documents nowadays contain provisions for testing at loading rates above the so-called "quasi-static regime". If we limit ourselves to current ASTM standards, we note the following, as a function of the mechanical response of the tested material.

→ Brittle behaviour (*lower shelf*): both the E399-90 and the E1820-01 standards prescribe a range of increase of stress intensity factor between 0.55 and 2.75 MPa√m/s. Above this upper limit, the user is redirected to Annex A7 (E399) or Annex A13 (E1820), but in both cases the requirements given do not "*include impact or quasi-impact testing (free-falling or swinging masses).*"

→ Ductile-to-brittle transition regime: the current version of E1921 (2005) limits the loading rate to 2 MPa√m/s; below this limit, the influence of loading rate on the reference temperature is expected to be less than 10 °C. No specific provisions are given for higher loading rates, although an Annex is currently in preparation within the responsible ASTM committee which should eventually cover high-rate tests (including precracked Charpy tests). Several investigations [1,2,3] have shown that the Master Curve analysis is however fully applicable to fracture toughness data obtained under dynamic conditions; a semi-empirical correlation between the increase of T_o and the loading rate has also been established [1].

→ Ductile behaviour (*upper shelf*): the E1820-01 standard contains an Annex (A14) titled "*Rapid-load J-integral Fracture Toughness Testing*", which is applicable when the loading rate exceeds the value allowed for conventional (static) testing, which corresponds to reaching the load P_f (used for fatigue precracking) in 0.1 min. However, limitations are imposed to the maximum tolerable oscillations in the elastic portion of the force/displacement trace, which are generally incompatible with an actual instrumented impact test on a precracked Charpy specimen.

Two other widely used fracture toughness test standards cannot in principle be applied to impact-tested PCCv specimens: ISO 12135:2002 (which is restricted to quasi-static loading rates up to 3 MPa√m/s) and BS 7448 Part 3 (which can be used for loading rates up to 3000 MPa√m/s).

In the upper shelf regime, the most commonly used method for determining ductile crack initiation and the crack resistance curve is the multiple-specimen technique, whereby each

sample provides one *J-Δa* point and the different specimens are tested up to varying amounts of ductile crack extension.

Two approaches can be used for obtaining different degrees of crack propagation:

- the low-blow test, in which each specimen is tested at a different velocity and with different potential energy, but in all cases such as not to fully break the sample;
- the stop block test, where the different amounts of crack extension are obtained by varying the arrest position of the striker, but again avoiding complete fracture of the specimen.

Both these techniques are described in the Test Procedure which is being developed by the ESIS Technical Committee 5 [4]. The multiple-specimen technique is regarded as the reference method.

Because of the nature of the impact test itself, the use of more conventional single-specimen techniques, such as Unloading Compliance or Potential Drop, is not feasible. However, new analytical approaches to the analysis of an individual force/deflection trace have recently surfaced:

→ the Normalization Data Reduction (NDR) technique, which is fully described in Annex A15 of E1820-01 and Annex 4 of the ESIS TC5 Test Procedure;

→ the Analytical 3-Parameter Approach, proposed by Schindler and included in Annex 4 of the ESIS TC5 Test Procedure;

→ a model proposed by R. Chaouadi and developed in 2003 for the Tractebel/SCK•CEN Convention.

The purpose of this investigation is to assess the applicability and reliability of these analytical single-specimen techniques for the determination of upper shelf dynamic toughness properties, based on the comparison with results obtained using the more conventional multiple-specimen (low-blow test) technique. Indeed, it is desirable to validate a single-specimen technique which would be effectively applicable to dynamic J-R measurements in the upper shelf regime without having to use the material-consuming multiple-specimen approach.

2 Materials and experimental

Two well characterized RPV steels, with clearly different mechanical properties, have been selected for this investigation.

The DIN 20MnMoNi55 steel comes from a forged boiler bottom segment, and its chemical composition (shown in Table 1) is similar to A533B Cl.1. Its main mechanical properties [5] are given in Table 2.

Table 1 - Chemical composition of 20MnMoNi55 (weight % - Fe balance).

C	Si	Mn	S	P	Cr	V	Cu	Al	Ni	Mo	Sn	Co	As	Sb	Ti
0.19	0.2	1.29	0.008	0.007	0.12	0.02	0.11	0.015	0.8	0.53	0.012	0.014	0.03	0.03	0.05

Table 2 - Main mechanical properties of 20MnMoNi55 [5].

R_{p02} (MPa)	R_m (MPa)	ε_u (%)	ε_t (%)	RA (%)	T_{41J} (°C)	T_{68J} (°C)	USE (J)	FATT (°C)	$T_{0.89mm}$ (°C)	T_o (°C)
429	576	11	22	73	-76	-58	181	-24	-68	-126

LEGEND

R_{p02}, R_m, ε_u, ε_t, RA = yield strength, tensile strength, uniform elongation, total elongation and reduction of area (at RT)

T_{41J}, T_{68J}, FATT, $T_{0.89mm}$ = temperatures corresponding to 41J and 68J absorbed energy, 50% shear fracture appearance and 0.89 mm lateral expansion from Charpy tests
T_o = quasi-static reference temperature measured on PCCv specimens with the Master Curve methodology.

The other material, JSPS, is a Japanese RPV steel of the A533B type, deliberately embrittled by increasing the concentration of S and P to simulate the degradation in toughness caused by neutron exposure. This steel was used by the Japan Society for the Promotion of Science (hence the name) in a Round-Robin exercise on fracture toughness measurements using Compact Tension specimens [6]. Its chemical composition and main mechanical properties are shown in Table 3 and Table 4, respectively.

Table 3 - Chemical composition of JSPS (weight % - Fe balance).

C	Si	Mn	S	P	Cr	Cu	Ni	Mo
0.24	0.41	1.52	0.023	0.028	0.08	0.19	0.43	0.49

Table 4 - Main mechanical properties of JSPS [6].

R_{p02} (MPa)	R_m (MPa)	ε_u (%)	ε_t (%)	RA (%)	T_{41J} (°C)	T_{68J} (°C)	USE (J)	FATT (°C)	$T_{0.89mm}$ (°C)	T_o (°C)
461	639	11	18	59	34	101	72	43	40	-7

For both materials, low-blow impact tests have been performed on fatigue precracked Charpy specimens using an instrumented striker conforming to the ISO 14556:2000 standard (tup radius = 2 mm). Tests have been executed at two different temperatures: RT (23 °C) and 290 °C for 20MnMoNi55; 100 and 290 °C for JSPS. All tested specimens were plain-sided.

Individual test results are collected in Table 5 for 20MnMoNi55 and Table 6 for JSPS. Annex 1 and Annex 2 contain the instrumented Charpy reports.

Table 5 - Results of the low-blow tests performed on PCCv specimens of the 20MnMoNi55 steel.

Specimen code	T (°C)	B (mm)	W (mm)	a_o (mm)	v_o (m/s)	E_p (J)	KV (J)	Δa (mm)	J (kJ/m²)	$\dot{J}$ [kJ/(m²·s)]
MMN-1113-L	23	9.919	9.957	5.038	0.99	10.01	9.13	0.256	369.17	1.045E+5
MMN-1009-R		9.914	9.953	5.112	1.20	14.94	13.87	0.368	558.17	1.380E+5
MMN-1006-R		9.900	9.936	5.251	1.40	20.04	18.64	0.535	774.72	1.679E+5
MMN-1009-L		9.956	9.967	5.202	1.57	25.02	23.42	1.050	916.63	1.728E+5
MMN-1114-L		9.904	9.934	5.172	1.72	29.98	28.13	1.302	1088.12	1.915E+5
MMN-1007-R		9.931	9.945	5.300	1.80	33.14	31.43	1.605	1208.73	1.871E+5
MMN-1002-R		9.926	9.967	5.043	1.88	36.14	34.30	1.787	1235.20	1.925E+5
MMN-1111-R		9.940	9.923	5.439	1.99	40.15	38.97	2.452	1428.51	1.506E+5
MMN-1003-L	290	9.867	9.940	5.026	0.99	9.97	9.49	0.347	372.19	0.897E+5
MMN-1007-L		9.928	9.962	5.281	1.22	15.07	14.45	0.539	577.69	1.136E+5
MMN-1002-L		9.913	9.936	5.018	1.40	20.04	19.24	0.601	741.70	1.435E+5
MMN-1112-R		9.909	9.952	5.261	1.57	25.02	24.03	0.871	970.15	1.674E+5
MMN-1113-R		9.942	9.957	5.164	1.71	29.92	28.93	1.238	1111.06	1.759E+5
MMN-1006-L		9.898	9.956	4.908	1.85	34.72	33.54	1.608	1217.62	1.710E+5
MMN-1003-R		9.886	9.932	5.128	1.92	37.65	36.77	2.412	1347.86	1.463E+5

Table 6 - Results of the low-blow tests performed on PCCv specimens of the JSPS steel.

Specimen code	T (°C)	B (mm)	W (mm)	a_o (mm)	v_o (m/s)	E_p (J)	KV (J)	Δa (mm)	J (kJ/m²)	$\dot{J}$ [kJ/(m²·s)]
JSP6_1	100	9.945	10.002	5.401	0.89	8.08	7.43	0.511	311.93	0.823E+5
JSP6_2		9.932	10.080	5.309	1.09	12.06	11.16	0.573	450.46	1.085E+5
JSP6_3		9.946	9.973	5.457	1.25	15.96	15.38	1.781	569.70	0.860E+5
JSP6_4		9.935	10.000	5.360	1.40	20.08	19.74	2.855	644.93	0.650E+5
JSPS-4-2-25-A	290	9.966	10.069	5.656	0.78	6.19	9.49	0.351	251.09	0.606E+5
JSPS-1-1-27-A		10.000	10.002	4.929	0.89	8.02	14.45	0.587	277.74	0.697E+5
JSPS-4-2-1-A		9.885	9.943	5.347	0.89	8.02	19.24	1.011	303.66	0.702E+5
JSPS-4-2-20-A		10.050	10.050	5.459	1.09	12.06	24.03	1.561	434.27	0.748E+5
JSPS-502-L		9.897	9.940	5.149	1.20	14.94	14.35	2.036	515.37	0.813E+5
JSPS-506-L		9.945	9.962	5.294	1.30	17.31	16.80	2.206	588.16	0.842E+5
JSPS-507-L		9.837	9.919	5.181	1.34	18.40	17.98	2.789	606.59	0.707E+5

LEGEND
B, W , a_o = specimen thickness, specimen width and initial crack length; v_o = impact velocity; E_p = potential energy; KV = absorbed energy; Δa = measured ductile crack extension; J = value of J-integral at test termination; $\dot{J}$ = loading rate, obtained dividing J by the time at test termination.

Test results have been analyzed in accordance with the ASTM E1820-01 standard for the obtainment of the critical J-integral value at initiation and the crack resistance curve. In the analyses, a correction for crack growth has been applied to the multiple-specimen J values, for consistency with single-specimen techniques (incremental formula for calculating J). For this purpose, use has been made of a recent proposal by K. Wallin [7], which should be incorporated in the forthcoming revision of E1820. In the analysis of dynamic data, tensile properties measured from dynamic tensile tests at relevant strain rates have been used.

The results of the multispecimen analyses are given in Table 7 (critical J values – $J_{0.2mm}$ and J_Q) and Figure 1 to Figure 4 (J-R curves). In both the Table and the Figures, a comparison is presented between dynamic and quasi-static J-R curves for the different materials and temperatures; the static curves were obtained using the Unloading Compliance method. An increase of initiation toughness and tearing resistance with increasing loading rate is quite visible in all instances, as expected on the basis of available literature on the topic [8]. A tendency of loading rate effects to be more pronounced at higher temperatures is also observed; attempting an interpretation of this trend is however outside the scope of this work.

The results presented fully confirm the large difference in upper shelf toughness between the two RPV steels.

Annex 3 (20MnMoNi55) and Annex 4 (JSPS) report detailed J-integral calculations for all specimens tested.

Table 7 - Critical J-integral values obtained from the analysis of multiple-specimen (dynamic, low-blow) and single-specimen (quasi-static) tests.

Material	T (°C)	Loading rate	$J_{0.2mm}$ (kJ/m²)	J_Q (kJ/m²)
20MnMoNi55	23	Dynamic	376.2	921.8
		Quasi-static	259.9	593.9
	290	Dynamic	314.4	1117.3
		Quasi-static	211.7	331.3

Material	T (°C)	Loading rate	$J_{0.2mm}$ (kJ/m²)	J_Q (kJ/m²)
JSPS	100	Dynamic	265.8	366.1
		Quasi-static	170.3	210.7
	290	Dynamic	172.9	253.2
		Quasi-static	68.8	79.2

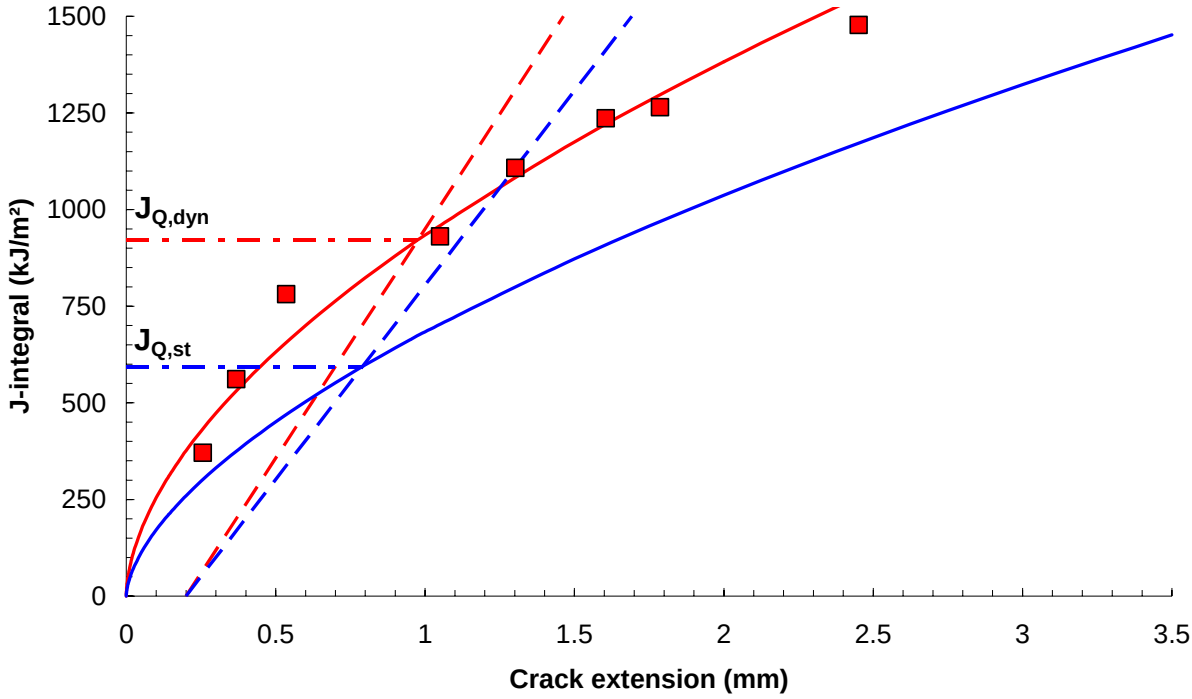

Figure 1 - Dynamic (red) and quasi-static (blue) J-R curves obtained on 20MnMoNi55 at RT.

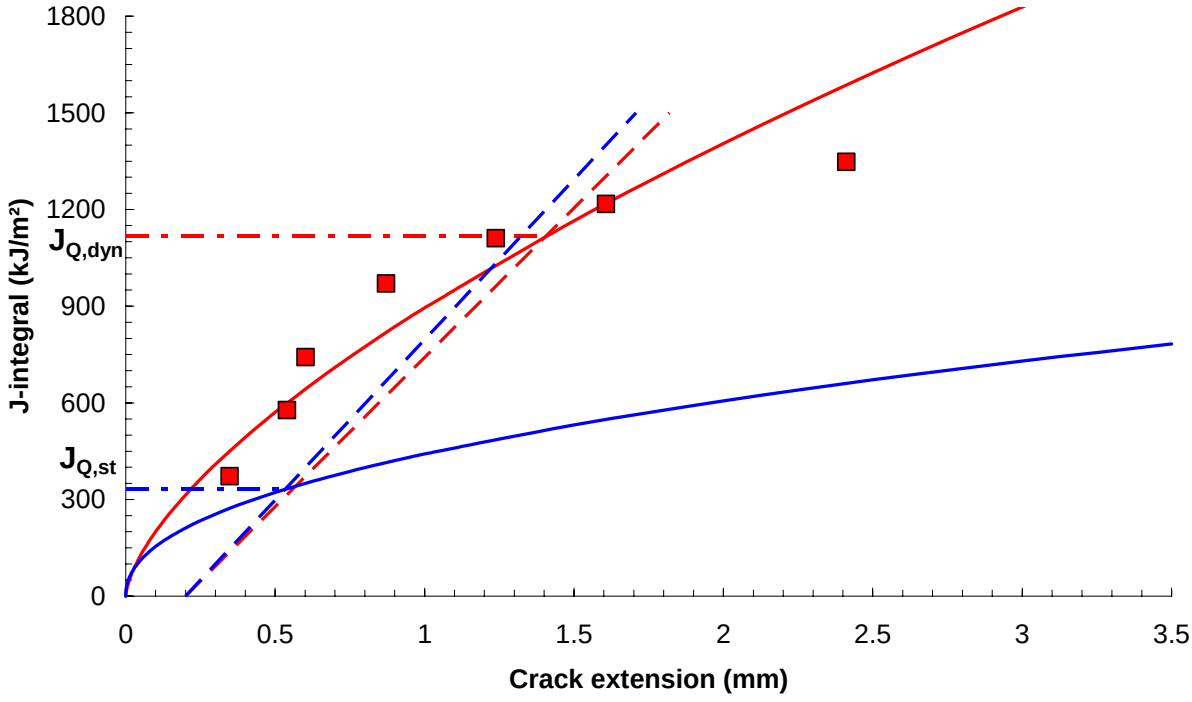

Figure 2 - Dynamic (red) and quasi-static (blue) J-R curves obtained on 20MnMoNi55 at 290 °C.

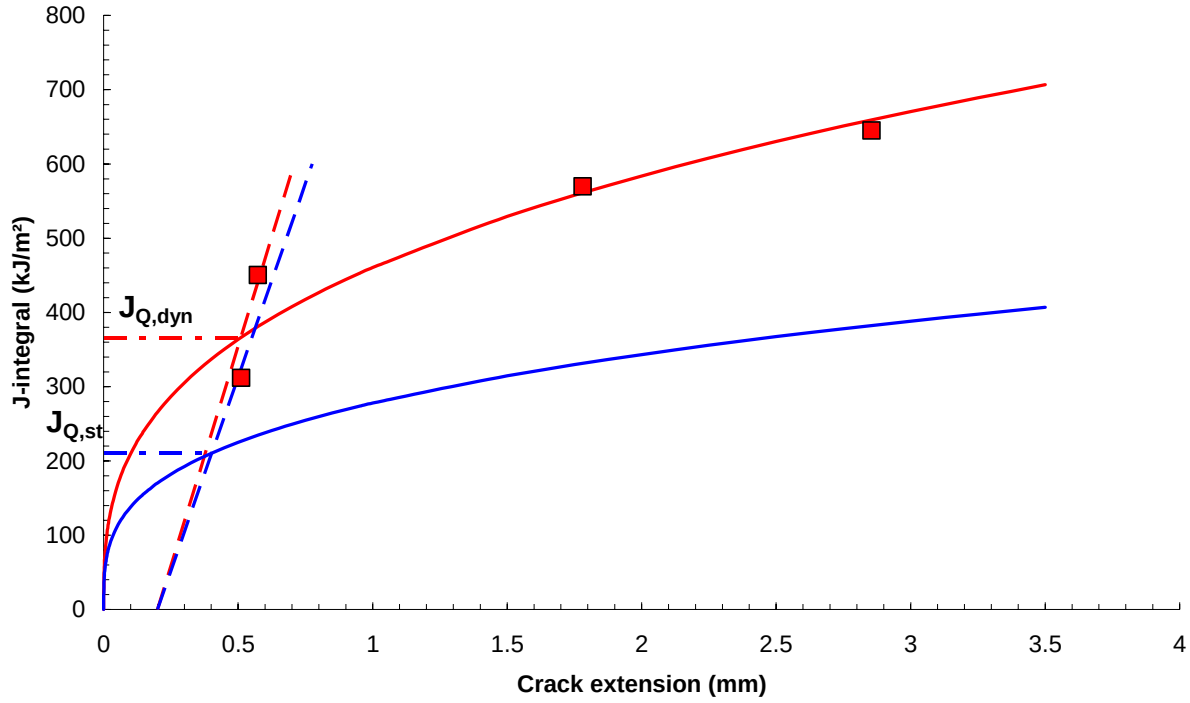

Figure 3 - Dynamic (red) and quasi-static (blue) J-R curves obtained on JSPS at 100 °C.

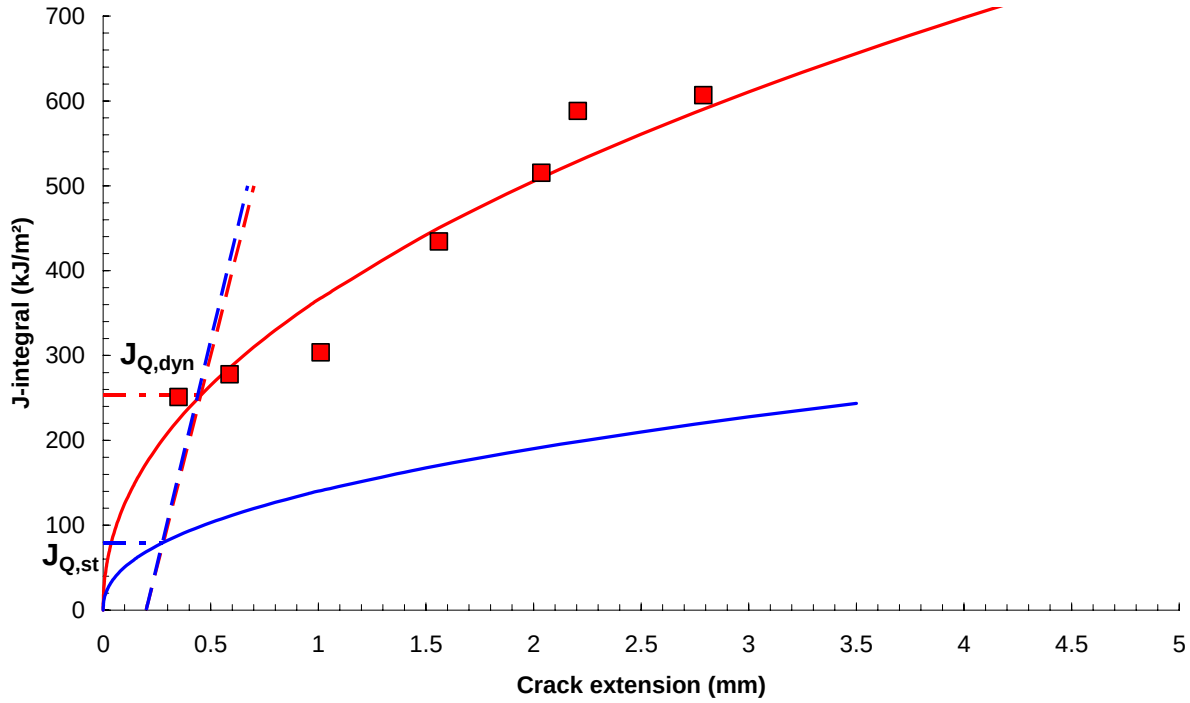

Figure 4 - Dynamic (red) and quasi-static (blue) J-R curves obtained on JSPS at 290 °C.

Among the low-blow tests reported in Table 7, only those with ductile crack growth larger than ~1.2 mm have been analyzed using the single-specimen methods described in the following chapter.

3 Single-specimen analyses of low-blow tests

3.1 Pre-treatment of the force/deflection traces: double fitting procedure

In order for an instrumentred trace to be amenable to the calculations detailed below and minimise the "noise" on the resulting J-R curve, a limited number of force/deflection data pairs must be selected for the analysis and the dynamic oscillations superimposed to the trace have to be smoothed out.

For this purpose, the instrumented trace of each test has been replaced by an idealized force/deflection diagrams, obtained through the following steps:

(a) the linear elastic portion has been fitted by a straight line up to the force at general yield F_{gy}, not accounting for the initial inertia peak;

(b) the subsequent part of the curve (from F_{gy} to the data point corresponding to zero velocity) has been fitted by a fourth-order[1] polynomial;

(c) a discrete number of data points to be used for further analysis have been selected on the two fitting lines, namely:
- → 4 data points[2] in the linear elastic portion, equi-spaced between 0 and F_{gy} (the last one coinciding with F_{gy});
- → 40 data points[2] in the plastic part of the curve, equi-spaced between F_{gy} and the end of the test (corresponding to v = 0).

An illustration of the procedure described above is shown in Figure 5.

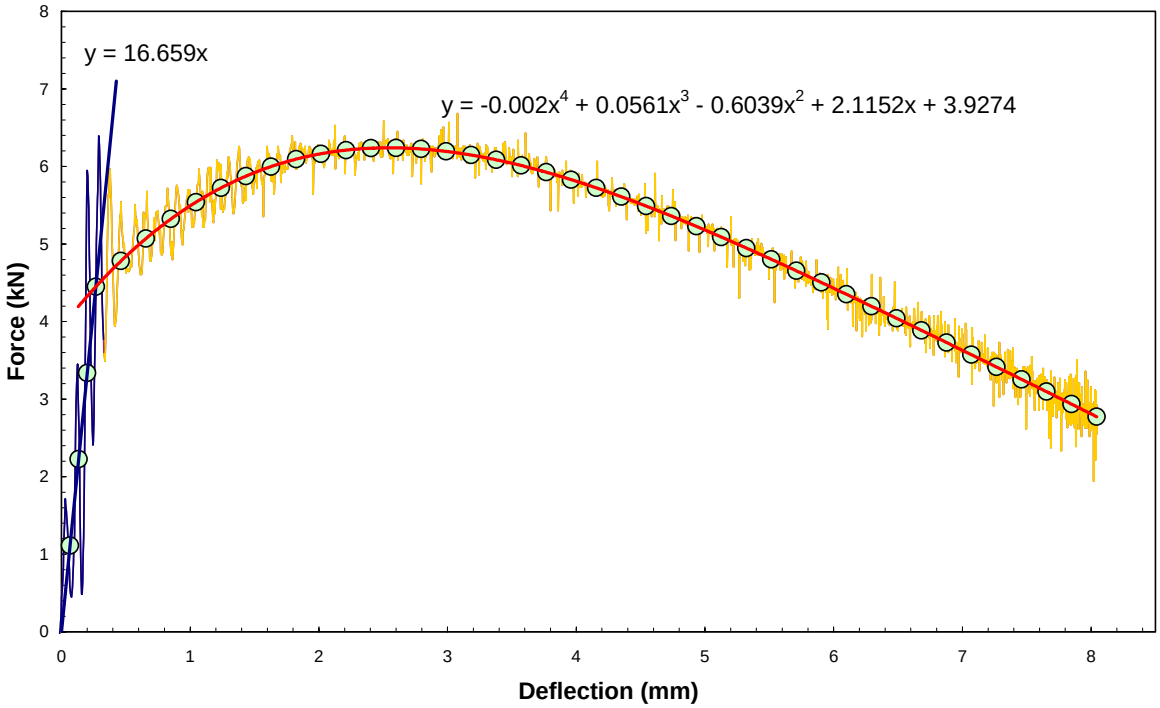

Figure 5 - Specimen MMN-1111_R (20MnNiMo55, RT): selection of the data points for the single-specimen analyses.

[1] In a few cases, polynomials of higher order (up to 6th) had to be used to obtain a satisfactory fitting.
[2] The choice of 4 data points in step 1 and 40 in step 2 is purely arbitrary. A smaller or higher number of data points is not expected to influence the end results.

3.2 The Normalization Data Reduction (NDR) technique

The NDR technique allows deriving a J-R curve directly from a force/displacement record, together with initial and final crack size measurements taken from the specimen fracture surface. It is particularly suited to instances where crack size monitoring during the tests (for example via compliance measurements) is not feasible, such as tests at high loading rates. It is based on the principle of load separation developed by Ernst et al [9] and has been exaustively described and validated for quasi-static upper shelf toughness tests on both C(T) and PCCv specimens in a previous investigation [10].

The methodology cannot be used on fully broken specimens, i.e. when $(W - a_o) = 0$, since normalized force values would tend to infinite; as a consequence, dynamic J-R curves can only be obtained from low-blow (or stop block) tests.

The results obtained using the NDR technique on selected specimens are given in Table 8 (critical J-integral values) and Figure 6 to Figure 9 (single-specimen J-R curves compared with the multi-specimen J-R curve). Detailed analyses performed using the NDR method are reported in Annex 5 (20MnMoNi55) and Annex 6 (JSPS).

Table 8 - Critical J-integral values obtained from the NDR analysis of selected low-blow tests, compared with the outcome of the multiple-specimen analysis.

Material	T (°C)	Specimen code	Δa (mm)	$J_{0.2mm}$ (kJ/m²)	J_Q (kJ/m²)
20MnMoNi55	23	MMN_1114_L	1.302	480.1	1016.3
		MMN_1007_R	1.605	595.0	1118.9
		MMN_1002_R	1.787	585.3	1082.0
		MMN_1111_R	2.452	416.5	922.7
		Average		**519.2**	**1035.0**
		Standard deviation		86.01	86.04
		Multiple-specimen		***376.2***	***921.8***
	290	MMN_1113_R	1.238	616.0	1089.2
		MMN_1113_R	1.608	437.6	1175.6
		MMN_1003_R	2.412	386.0	925.2
		Average		**479.9**	**1063.3**
		Standard deviation		120.69	127.17
		Multiple-specimen		***314.4***	***1117.3***
JSPS	100	JSP6_3	1.781	249.5	350.0
		JSP6_4	2.855	271.0	365.9
		Average		**260.2**	**357.9**
		Multiple-specimen		***265.8***	***366.1***
	290	4-2-20-A	1.561	160.2	232.3
		502_L	2.036	189.8	271.7
		506_L	2.206	212.9	327.0
		507_L	2.789	190.2	287.6
		Average		**188.3**	**279.6**
		Standard deviation		21.58	***39.23***
		Multiple-specimen		***172.9***	***253.2***

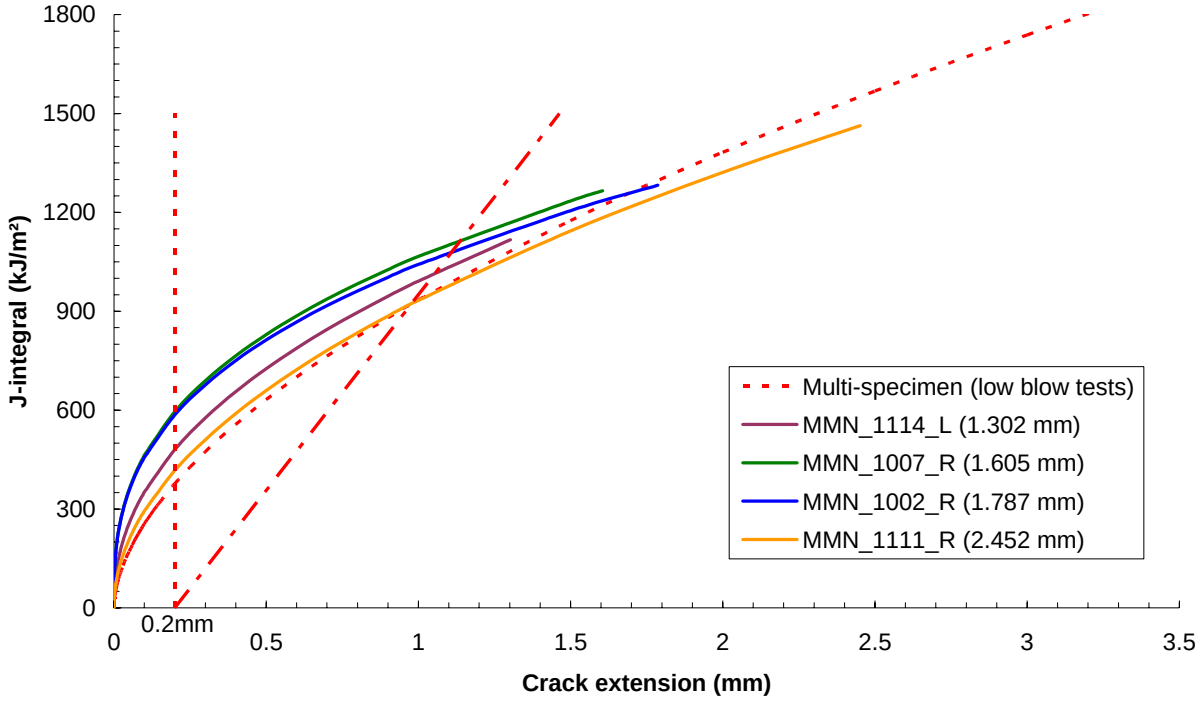

Figure 6 - Comparison between multiple-specimen (low-blow) and single-specimen (NDR) J-R curves for 20MnMoNi55 at RT.

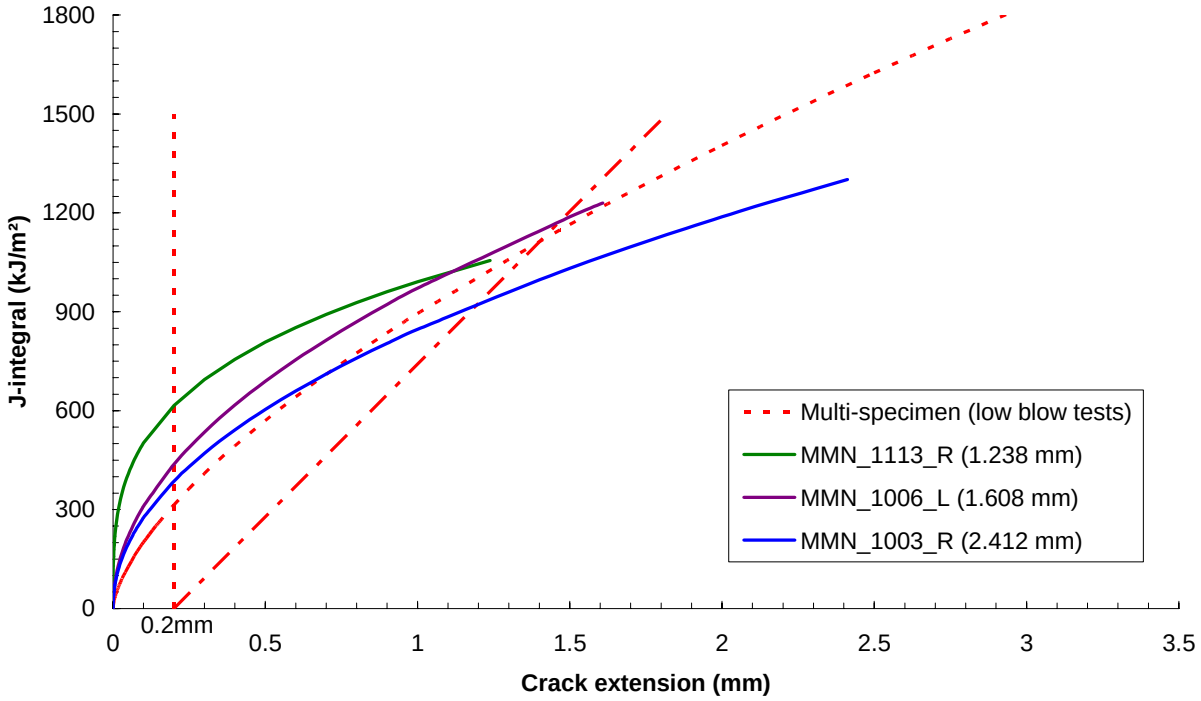

Figure 7 - Comparison between multiple-specimen (low-blow) and single-specimen (NDR) J-R curves for 20MnMoNi55 at 290 °C.

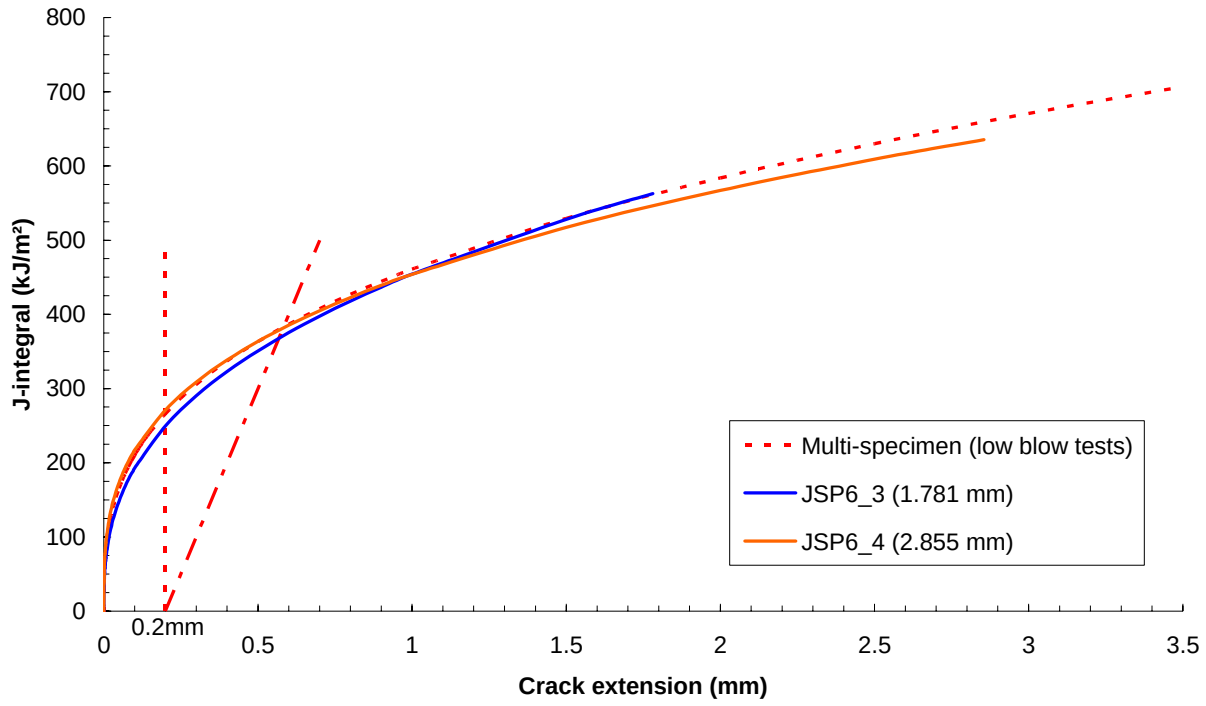

Figure 8 - Comparison between multiple-specimen (low-blow) and single-specimen (NDR) J-R curves for JSPS at 100 °C.

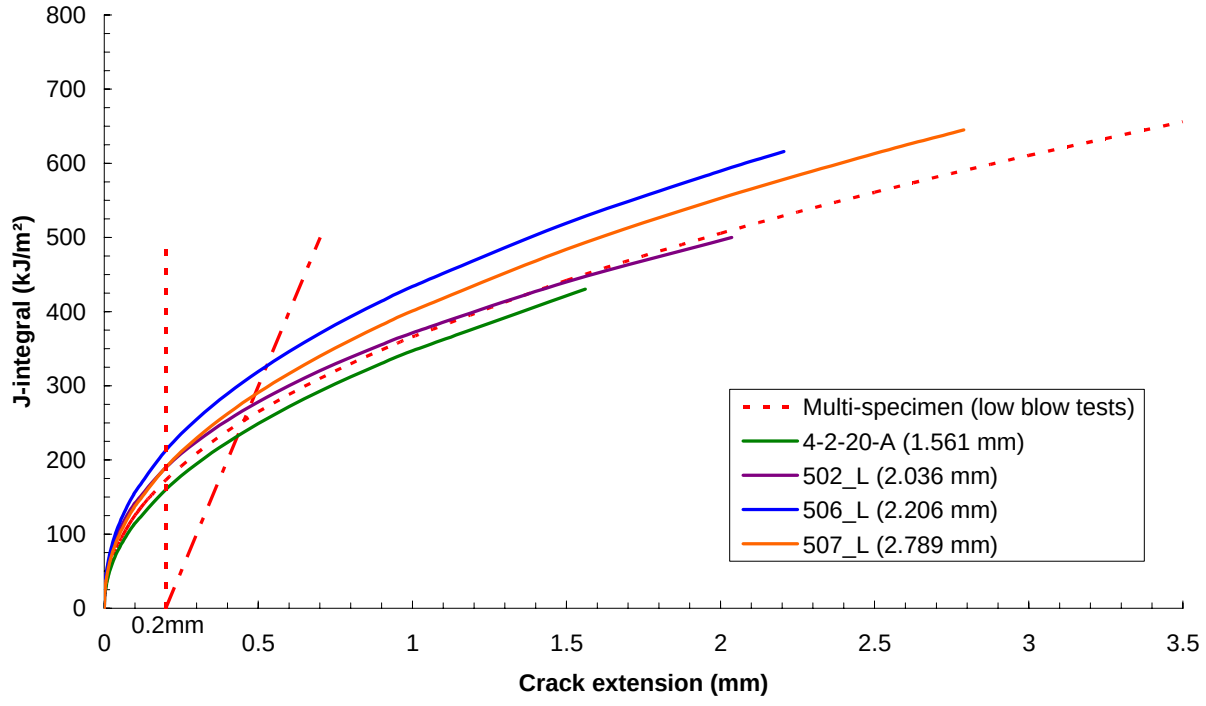

Figure 9 - Comparison between multiple-specimen (low-blow) and single-specimen (NDR) J-R curves for JSPS at 290 °C.

3.2.1 Discussion

The agreement between multiple (low blow) and single (NDR) specimen results ranges from acceptable (20MnMoNi55 at RT, Figure 6) to very good (JSPS at 100 °C, Figure 8). In terms of initiation parameters (J_Q) and considering mean values for the NDR analyses, differences range from -4.9% to +12.3%. Moreover, the multiple-specimen value is always within ±1σ (σ = standard deviation) from the average value of the single-specimen analyses.

The NDR technique, therefore, appears to be an effective method for deriving single-specimen J-R curves under dynamic loading conditions.

3.3 Analytical 3-parameter approach (Schindler's Key-Curve method)

An estimation method for the J-R curve, based on a continuous force-displacement diagram, has been proposed by Schindler [10,11] and is presently included in the latest draft of the ESIS TC5 Test Procedure [4].

The J-R curve is given by:

$$J = \frac{K_I^2}{E}\cdot\left(1-\nu^2\right)+\left(\frac{2}{p}\right)^p\cdot\frac{\eta}{B\left(W-a_o\right)^{1+p}}\cdot W_t^{\,p}\cdot W_{mp}^{\,1-p}\cdot\Delta a^p \qquad (1)$$

with:

$$K_I = \frac{2.659\cdot F_{gy}\cdot S}{\sqrt{BB_N}W^{3/2}}\cdot\left(\frac{a_i}{W}\right)^{1/2}\cdot\left[1.090-1.735\cdot\left(\frac{a_i}{W}\right)+8.2\cdot\left(\frac{a_i}{W}\right)^2-14.18\cdot\left(\frac{a_i}{W}\right)^3+14.57\cdot\left(\frac{a_i}{W}\right)^4\right] \qquad (2)$$

and:

$$p = \frac{3}{4}\cdot\left(1+\frac{W_{mp}}{W_t}\right)^{-1} \qquad (3)$$

where: W_t = total fracture energy; W_{mp} = plastic component of the energy up to maximum force; S = specimen span; a_i = current crack size ($a_i = a_o + \Delta a$).

Besides sample dimensions, this approach only requires knowlegde of F_{gy}, W_t and W_{mp} (3-parameter approach).

Eqs.(1-3) have been applied to the same low-blow tests already treated using the NDR technique. However, since the methodology is in principle applicable to fully broken specimens (unlike the NDR technique, as previously mentioned), an additional test on a fully broken specimen (4-2-2-A, JSPS, 290 °C) has been analysed.

Results compared to multiple-specimen data are reported in Table 9 (initiation values) and Figure 10 to Figure 13 (J-R curves). Detailed analyses are given in Annex 7 (20MnMoNi55) and Annex 8 (JSPS).

Table 9 - Critical J-integral values obtained from the application of Schindler's 3-parameter approach to selected low-blow tests, compared with the outcome of the multiple-specimen analysis.

Material	T (°C)	Specimen code	Δa (mm)	$J_{0.2mm}$ (kJ/m²)	J_Q (kJ/m²)
20MnMoNi55	23	MMN_1114_L	1.302	376.3	757.0
		MMN_1007_R	1.605	403.3	874.8
		MMN_1002_R	1.787	402.0	869.7
		MMN_1111_R	2.452	380.1	930.7
		Average		**393.9**	**833.8**
		Standard deviation		15.22	66.61
		Multiple-specimen		***376.2***	***921.8***
	290	MMN_1113_R	1.238	356.0	826.8
		MMN_1113_R	1.608	351.7	850.1
		MMN_1003_R	2.412	358.6	960.3
		Average		**353.9**	**838.4**
		Standard deviation		3.03	16.48
		Multiple-specimen		***314.4***	***1117.3***
JSPS	100	JSP6_3	1.781	164.5	238.9
		JSP6_4	2.855	188.3	292.2
		Average		**176.4**	**265.6**
		Multiple-specimen		***265.8***	***366.1***
	290	4-2-20-A	1.561	116.0	196.9
		502_L	2.036	151.4	206.1
		506_L	2.206	163.2	236.1
		507_L	2.789	158.4	275.2
		4-2-2-A (*)	4.745	155.8	212.4
		Average		**147.3**	**228.6**
		Standard deviation		21.39	35.29
		Multiple-specimen		***172.9***	***253.2***

NOTE – (*) Fully broken specimen (impact velocity: 1.57 m/s).

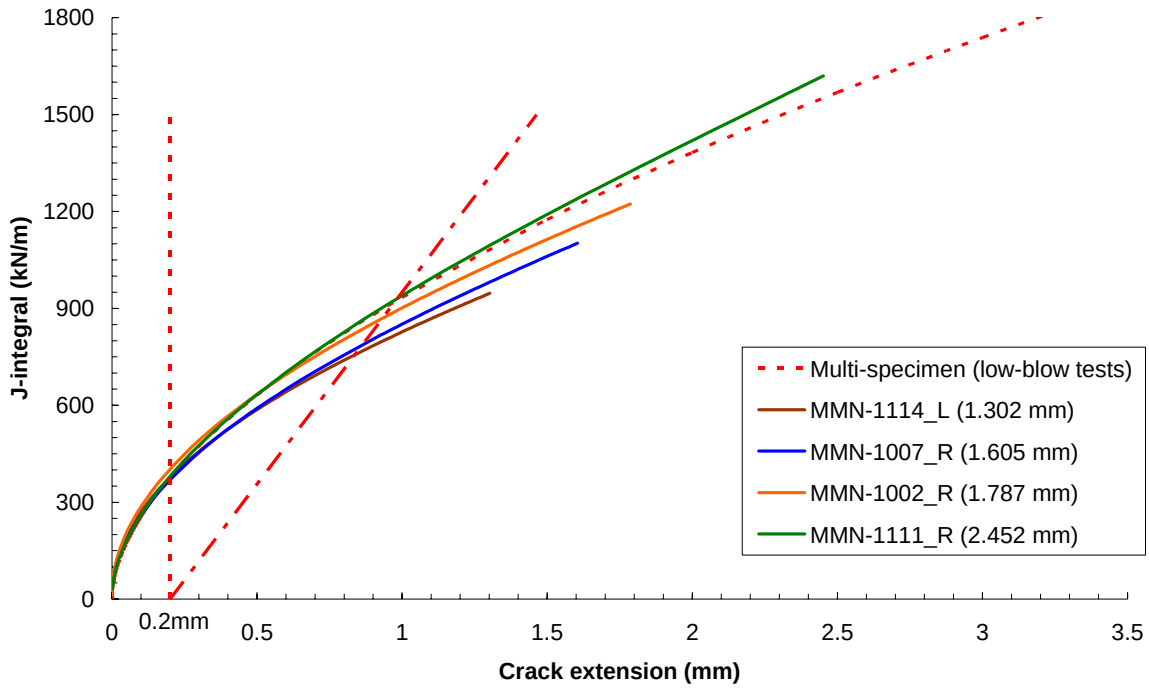

Figure 10 - Comparison between J-R curves obtained from the multiple-specimen (low-blow) and single-specimen (Schindler's key curve) approaches for 20MnMoNi55 at RT.

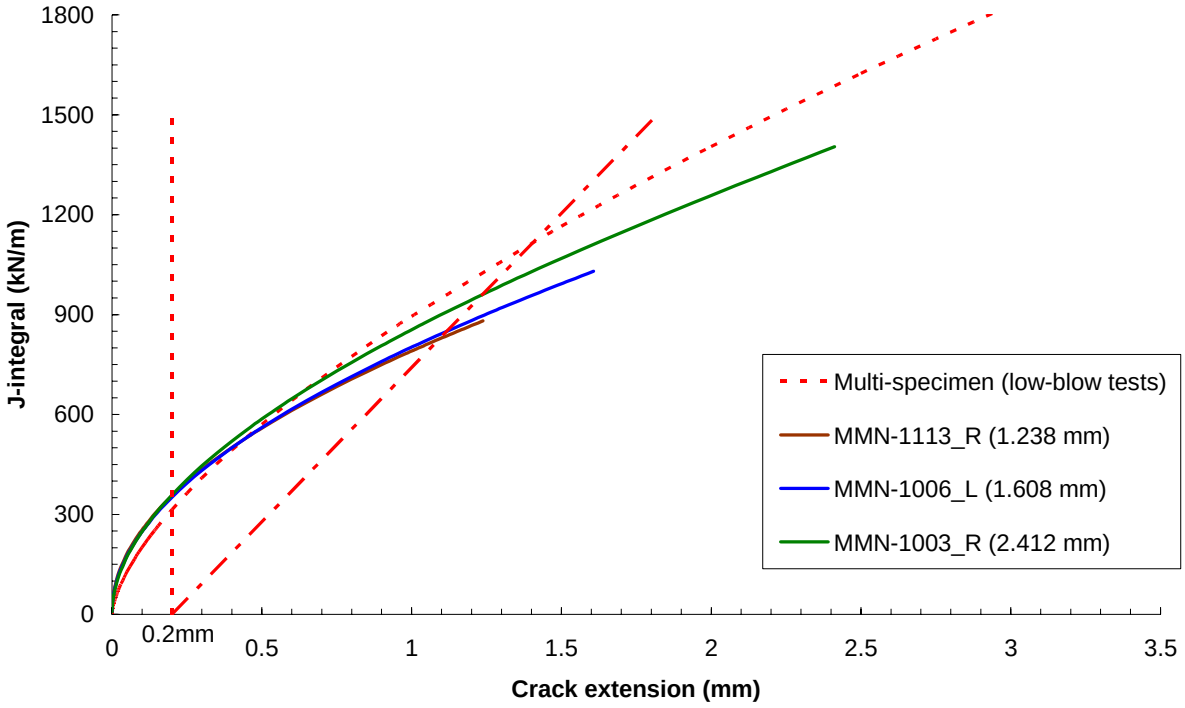

Figure 11 - Comparison between J-R curves obtained from the multiple-specimen (low-blow) and single-specimen (Schindler's key curve) approaches for 20MnMoNi55 at 290 °C.

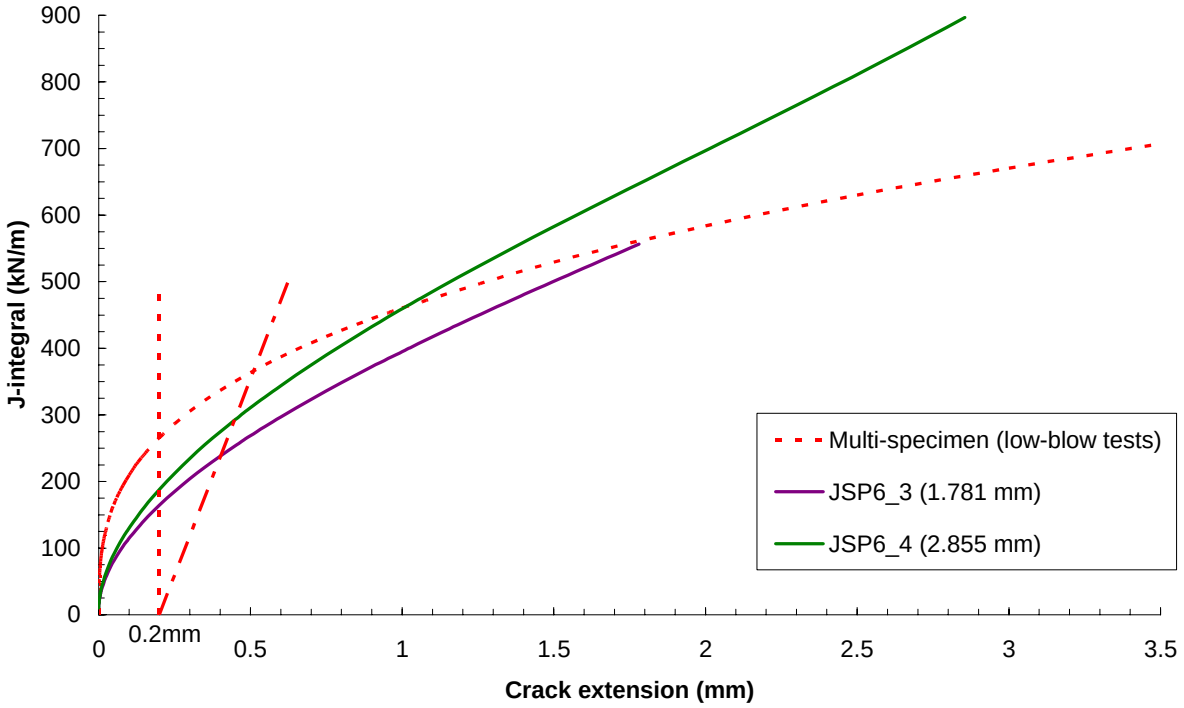

Figure 12 - Comparison between J-R curves obtained from the multiple-specimen (low-blow) and single-specimen (Schindler's key curve) approaches for JSPS at 100 °C.

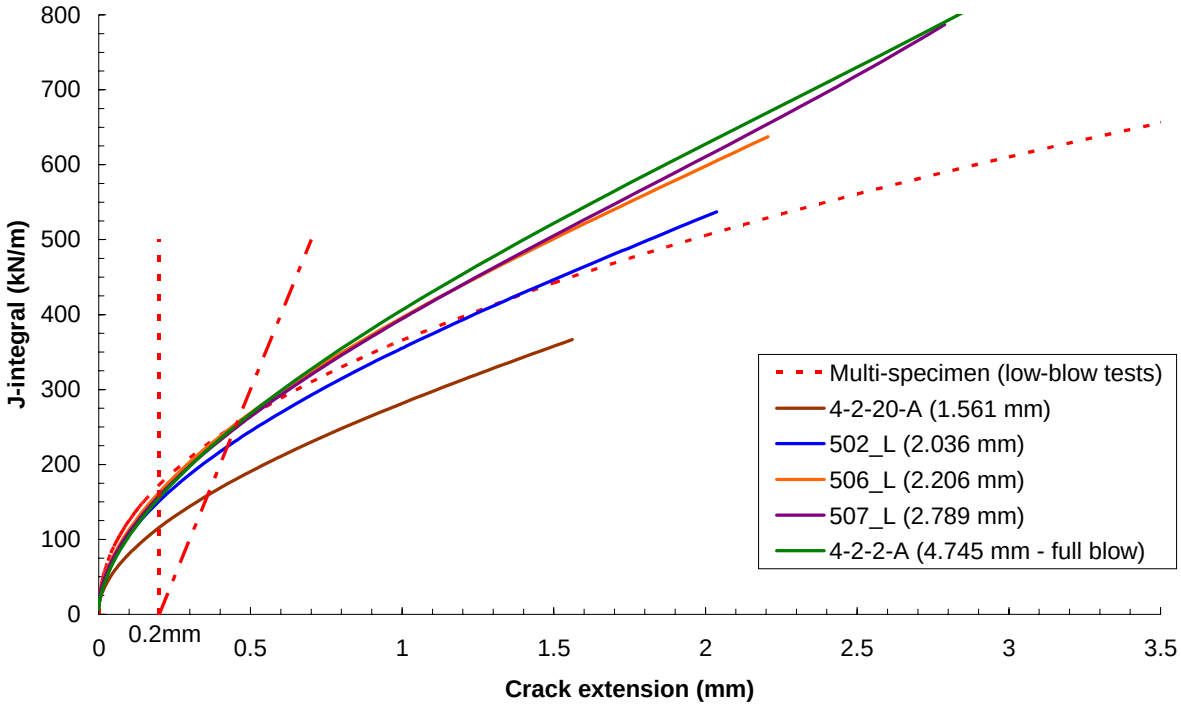

Figure 13 - Comparison between J-R curves obtained from the multiple-specimen (low-blow) and single-specimen (Schindler's key curve) approaches for JSPS at 290 °C.

3.3.1 Discussion

For Schindler's key curve approach, the overall agreement with the multiple-specimen results is good, although a tendency to underestimation is visible, particularly in the ductile initiation region. In terms of J_Q, the differences between multiple-specimen and single-specimen (mean value) range from -9.5% to -27.5%. The slope of the multiple-specimen crack resistance curve is better reproduced for 20MnMoNi55 than for JSPS; the scatter is somewhat lower than for the NDR technique.

This analytical method seems to provide a reasonable, tendentially conservative approximation of the toughness properties measured with the multiple-specimen approach.

3.4 Chaouadi's approach

Another analytical approach has been proposed by Chaouadi in the framework of the 2003 Tractebel/SCK•CEN Convention [12]. Like Schindler's method, it is purely based on the analysis of the force/displacement test record and can be in principle applied to any specimen geometry and loading rate.

At any point on the force/displacement trace, crack extension is related to the absorbed energy E via the following quadratic relationship:

$$\frac{\Delta a}{\Delta a_p} = \left(\frac{E - W_i}{W_t - W_i} \right)^2 \qquad (4)$$

where Δa_p is the measured total crack extension, W_t is the total absorbed energy and W_i is the absorbed energy at initiation. The evaluation of this latter parameter is based on the assumption that on the force/displacement trace, the onset of ductile tearing is located approximately midway between general yield and maximum force (Figure 14). In other words, $F_i \approx \frac{F_{gy} + F_m}{2}$ [13]. The absorbed energy corresponding to F_i is obviously W_i, to be used in eq (4).

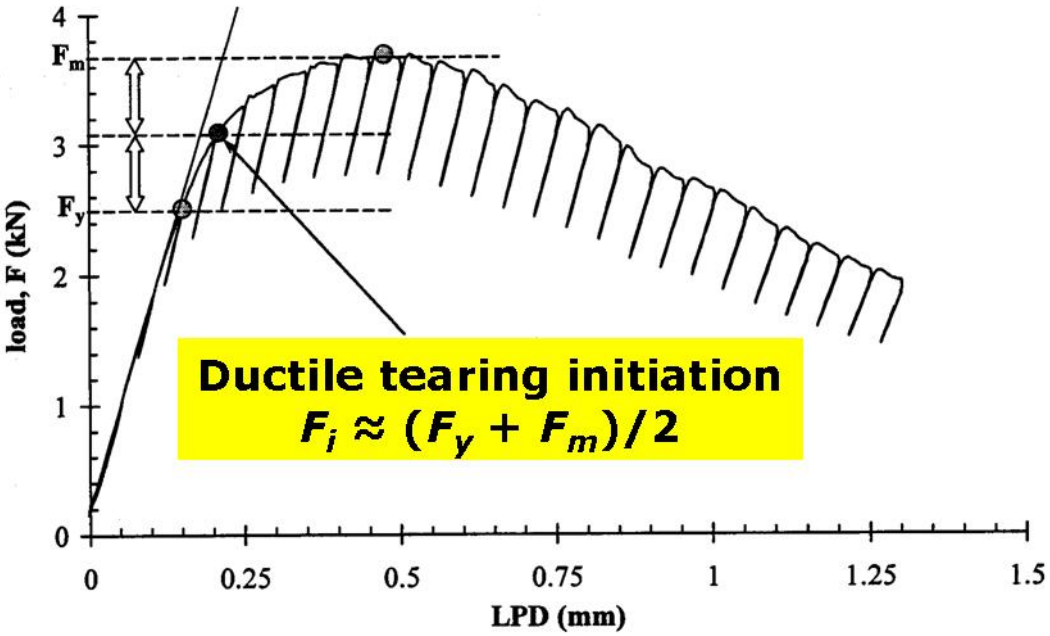

Figure 14 - Onset of ductile crack initiation on a generic force/displacement record [12,13].

The crack resistance curve can be expressed as:

$$J = J_i + J_t \sqrt{\Delta a} \tag{5}$$

where J_i, the initiation toughness, is given by:

$$J_i = \frac{\eta \cdot W_i}{B(W - a_o)} \tag{6}$$

and J_t, the tearing resistance, corresponds to:

$$J_t = \frac{\eta \cdot (W_t - W_i)}{B(W - a_o)\sqrt{\Delta a_p}} \tag{7}$$

Note that eq.(5) is not corrected for crack extension, thus to make it consistent with the remaining multiple- or single-specimen analyses, the following expression has been adopted:

$$J = \left(J_i + J_t \sqrt{\Delta a}\right) \cdot \left[1 - \frac{(0.75\eta - 1)\Delta a}{W - a_o}\right] \tag{8}$$

where the term between square brackets is the crack growth correction factor used in the ESIS P2-92 test procedure [14].

Note also that, with respect to the analytical approaches previously described, Chaouadi's method assumes a fixed value (0.5) for the power law exponent of the J-R curve, plus an offset (J_i).

The same tests already analysed according to Schindler's key curve have been considered, including the fully broken specimen from JSPS, tested at 290 °C.

Results are presented in Table 10 (initiation values) and Figure 15 to Figure 18 (J-R curves). More details on the calculations performed are given in Annex 9 (20MnMnMo55) and Annex 10 (JSPS).

Table 10 - Critical J-integral values obtained from the application of Chaouadi's method to selected low-blow tests, compared with the outcome of the multiple-specimen analysis.

Material	T (°C)	Specimen code	Δa (mm)	$J_{0.2mm}$ (kJ/m²)	J_Q (kJ/m²)
20MnMoNi55	23	MMN_1114_L	1.302	535.8	914.3
		MMN_1007_R	1.605	588.9	977.3
		MMN_1002_R	1.787	581.6	965.8
		MMN_1111_R	2.452	570.6	1031.6
		Average		**568.7**	**952.5**
		Standard deviation		28.79	33.55
		Multiple-specimen		***376.2***	***921.8***
	290	MMN_1113_R	1.238	525.3	1052.2
		MMN_1113_R	1.608	533.4	1040.0
		MMN_1003_R	2.412	511.5	977.2
		Average		**529.3**	**1046.1**
		Standard deviation		5.68	8.64
		Multiple-specimen		***314.4***	***1117.3***
JSPS	100	JSP6_3	1.781	261.5	363.2
		JSP6_4	2.855	281.4	385.2
		Average		**271.5**	**374.2**
		Multiple-specimen		***265.8***	***366.1***
	290	4-2-20-A	1.561	204.6	282.9
		502_L	2.036	215.7	300.1
		506_L	2.206	250.4	361.7
		507_L	2.789	242.4	345.0
		4-2-2-A (*)	4.745	288.3	376.9
		Average		**228.3**	**322.4**
		Standard deviation		21.69	37.01
		Multiple-specimen		***172.9***	***253.2***

NOTE – (*) Fully broken specimen.

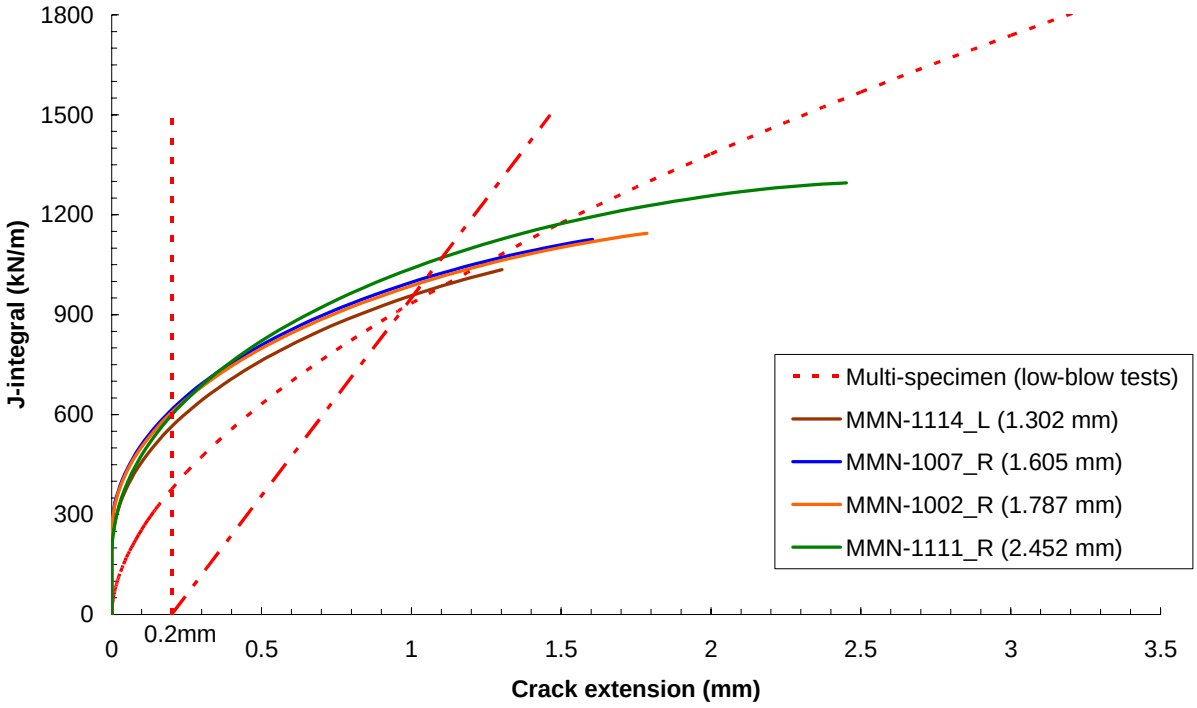

Figure 15 - Comparison between J-R curves obtained from the multiple-specimen (low-blow) and single-specimen (Chaouadi's method) approaches for 20MnMoNi55 at RT.

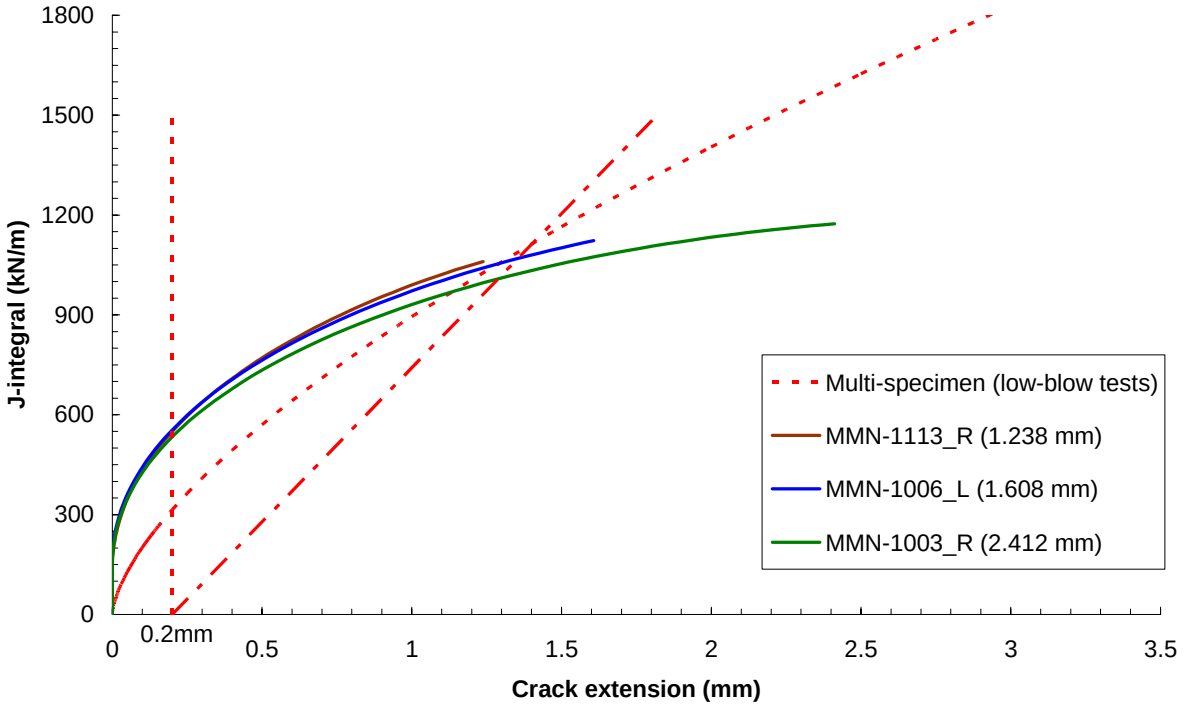

Figure 16 - Comparison between J-R curves obtained from the multiple-specimen (low-blow) and single-specimen (Chaouadi's method) approaches for 20MnMoNi55 at 290 °C.

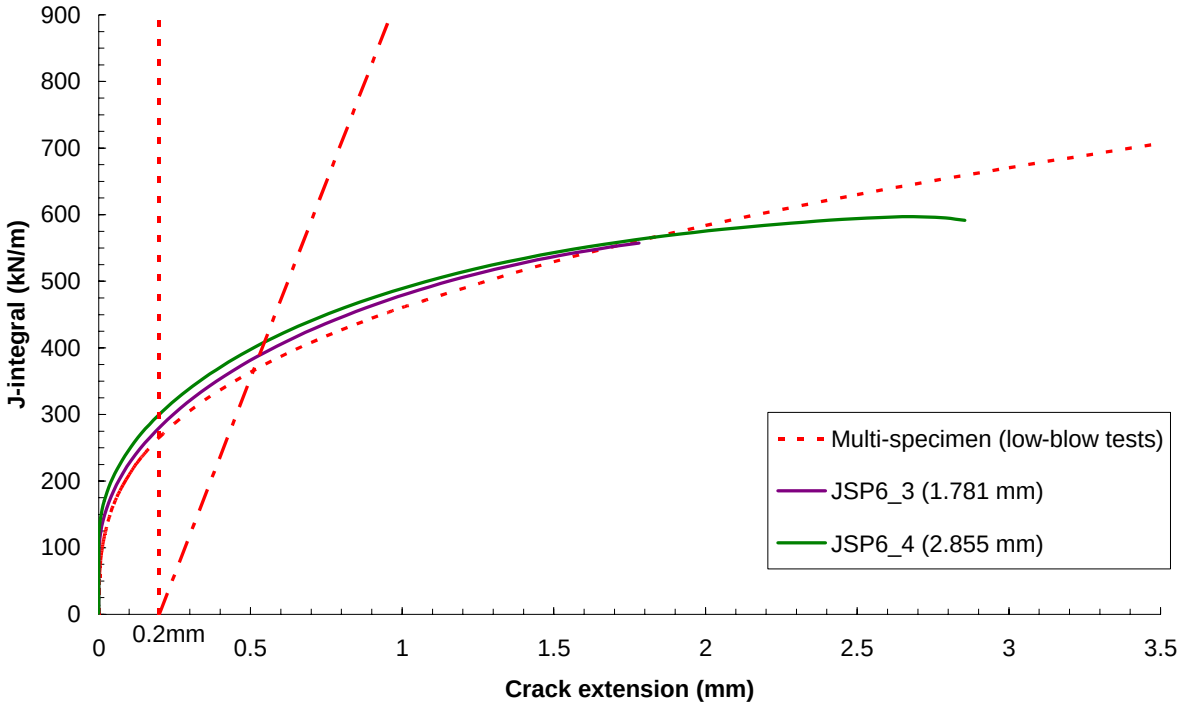

Figure 17 - Comparison between J-R curves obtained from the multiple-specimen (low-blow) and single-specimen (Chaouadi's method) approaches for JSPS at 100 °C.

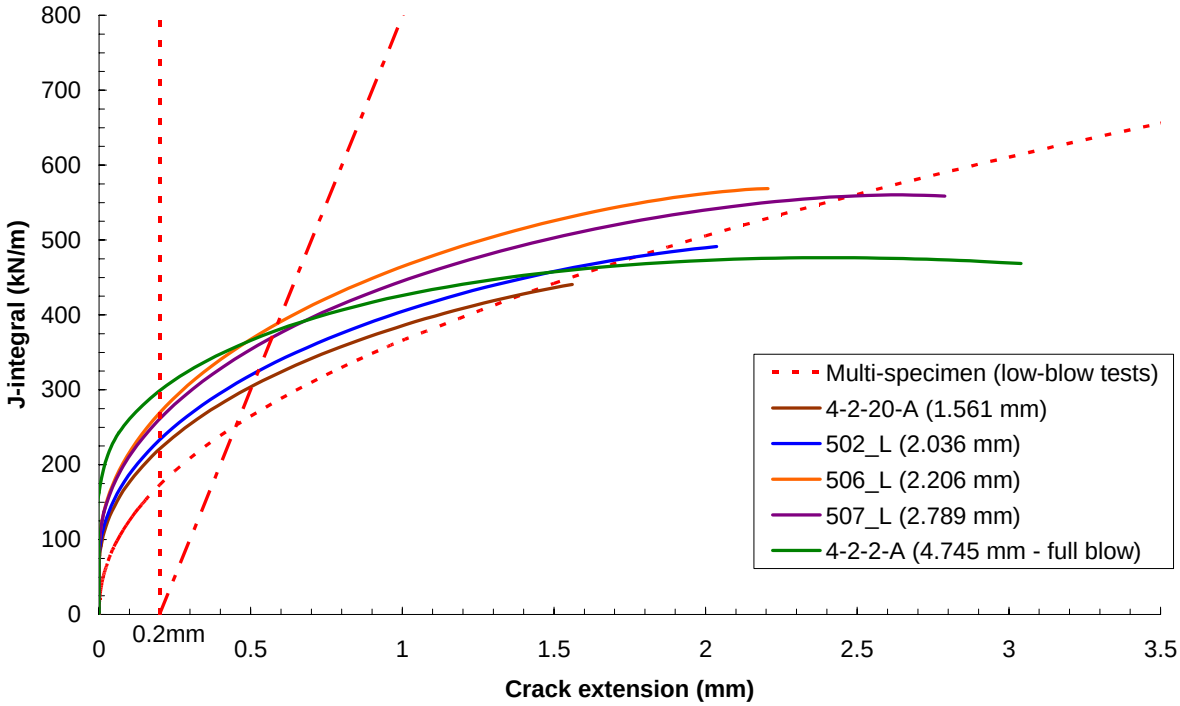

Figure 18 - Comparison between J-R curves obtained from the multiple-specimen (low-blow) and single-specimen (Chaouadi's method) approaches for JSPS at 290 °C.

3.4.1 Discussion

A fair agreement with the multiple-specimen results has been observed for the materials and temperatures investigated. The method seems however to provide non-conservative estimations of the critical parameters and the resistance curve.

The fixed value of the J-R curve exponent appears to be a limitation, which can yield significant discrepancies especially in the early stages of crack propagation (see for example 20MnMoNi55 at RT, Figure 15, and the values of $J_{0.2mm}$ in Table 10). In a couple of circumstances, the single-specimen and the multiple-specimen curves cross each other nearby the region where engineering initiation is defined (0.2 mm offset from the construction line), hence the very good agreement in terms of J_Q, which appears however coincidental: see for instance Figure 15 and Figure 16.

The overall scatter of the results seems to be smaller than for the other techniques investigated.

4 Overall comparative analysis and conclusions

In order to obtain an overall perspective of how effectively the individual single-specimen methods described in this report can represent the upper shelf behaviour under dynamic (impact) loading rates, we will consider not only critical the J-integral values ($J_{0.2mm}$ and J_Q), but also another parameter which is related to the resistance of the material to crack propagation.

A parameter which can give an indication of the relative stability of crack extension is the *tearing modulus* T_R, which is related to the slope of the J-R curve at a given value of Δa. It can be expressed in dimensionless terms as [15]:

$$T_R = \frac{E'}{\sigma_y}\left(\frac{dJ}{da}\right) \tag{9}$$

with E' = plane strain Young's modulus; T_R normally calculated at the point on the J-R curve which corresponds to J_Q. Since we will be comparing values of T_R for the same materials and temperatures, eq.(9) can be simplified to:

$$T = \left|\frac{dJ}{da}\right|_{\Delta a_Q} \tag{10}$$

where Δa_Q is the crack extension corresponding to J_Q and T is usually expressed in MPa.

In this analysis, like everywhere else in this report, the results of the multiple-specimen method will be assumed as the reference.

The comparisons between multiple and single-specimen approaches for the materials and temperatures investigated are shown in Figure 19 for $J_{0.2mm}$, Figure 20 for J_Q and Figure 21 for T.

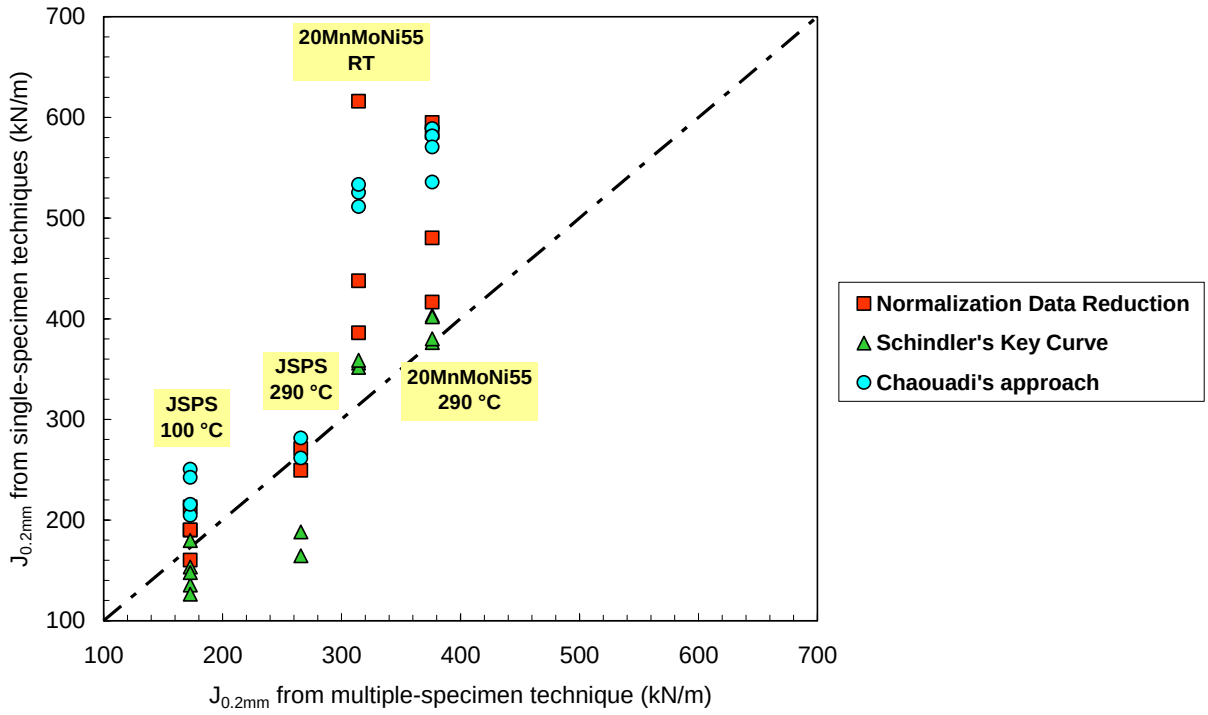

Figure 19 - Comparison between multiple and single-specimen results in terms of $J_{0.2mm}$.

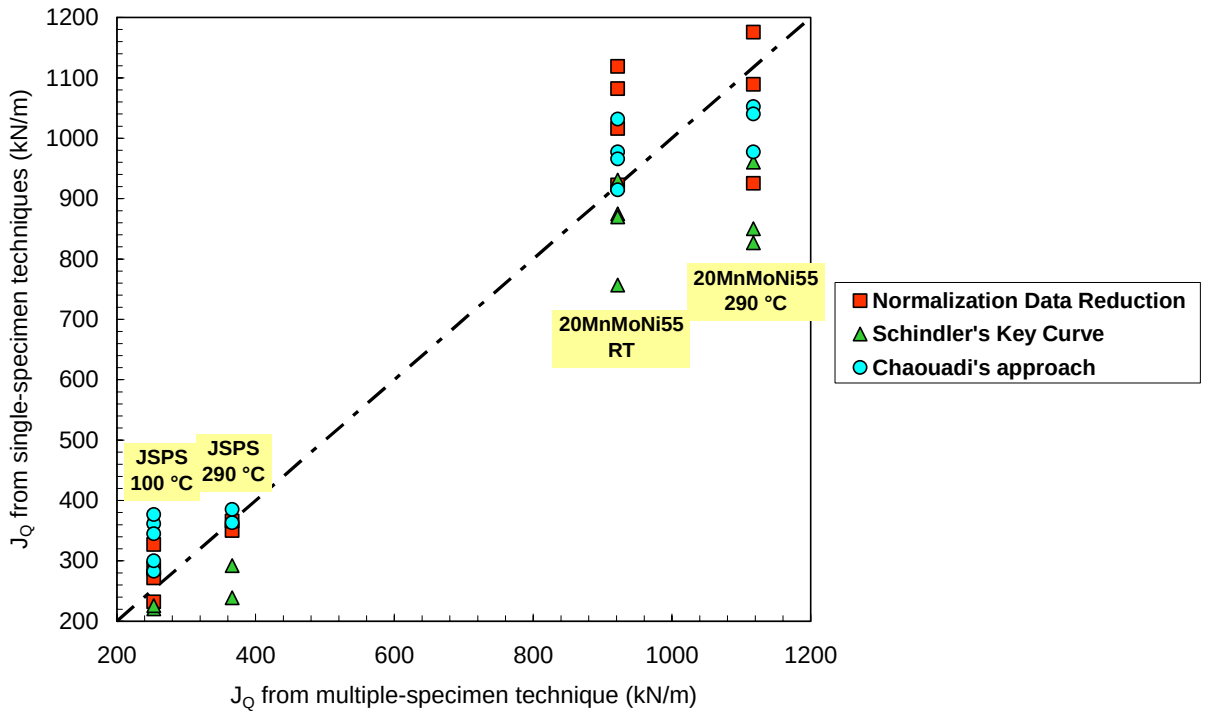

Figure 20 - Comparison between multiple and single-specimen results in terms of J_Q.

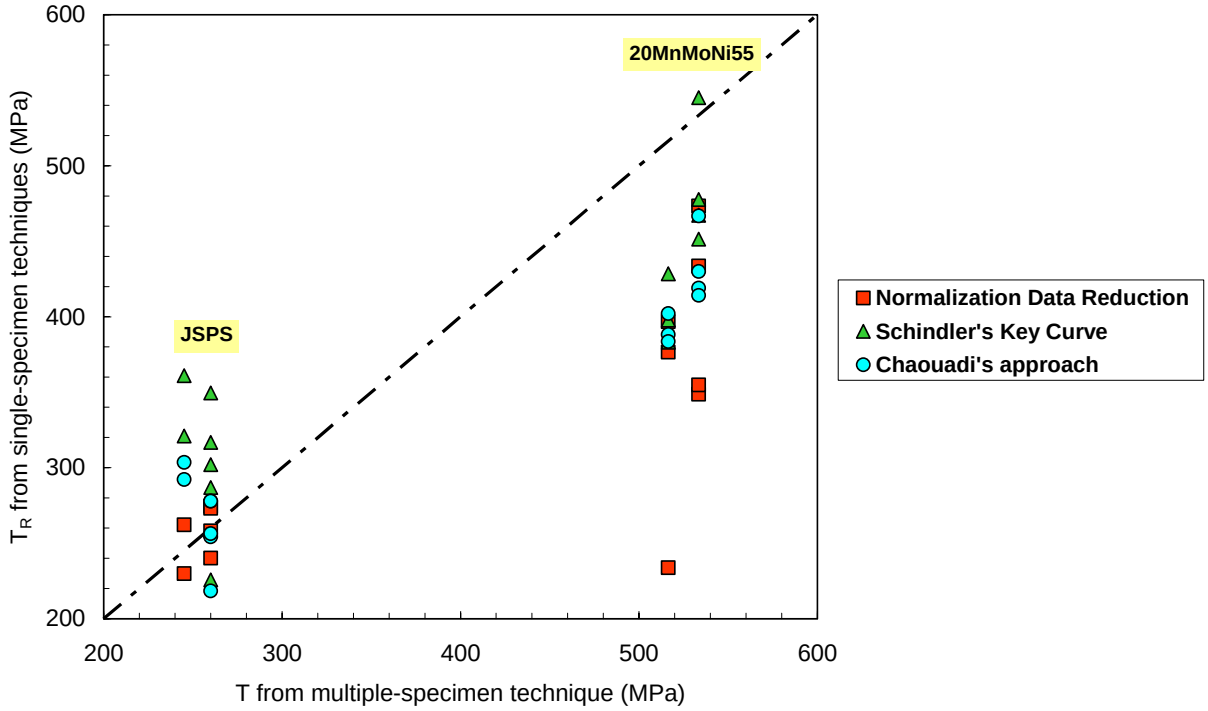

Figure 21 - Comparison between multiple and single-specimen results in terms of tearing modulus T_R.

It's not easy to pinpoint clear systematics in the results shown in Figure 19 to Figure 21. However, the following can be remarked.

(a) $J_{0.2mm}$ (Figure 19): the performance of the single-specimen approaches is better for the low toughness JSPS than for the high toughness 20MnMoNi55, for which the predictions are systematically higher than the reference. Schindler's key curve tends to provide lower end values, opposite to Chaouadi's method, which shows a tendency to overestimation; the NDR method is located somewhat in-between.

(b) J_Q (Figure 20): the accuracy of the single-specimen methods is acceptable for both materials, although the scatter for the high toughness 20MnMoNi55 is significant. For this latter material, it's the NDR technique which delivers the highest results; Schindler's key curve remains the most conservative.

(c) T_R (Figure 21): accuracy is quite poor for 20MnMoNi55, in that resistance to crack extension appears seriously underestimated for the single-specimen methods. Conversely, for JSPS the overall impression is a slight non-conservatism of the predicition, although within an acceptable scatterband. Consistently with what we remarked for initiation toughness values, Schindler's key curve tends to provide the steeper J-R curves.

The bottom line is that all three single-specimen approach are easily applicable to the analysis of the force-displacement curve of a PCCv specimen tested with an instrumented impact pendulum. They represent an acceptable alternative to the simpler but more material-consuming multiple-specimen method (low-blow or stop-block tests). However, in view of the experimental and analytical uncertainties, it is advisable to perform the analysis on a minimum of three specimens tested under the same conditions.

A general tendency to overestimation for Chaouadi's approach and to underestimation for Schindler's key curve has been observed. For this reason, and because of its more robust theoretical background, the use of the Normalization Data Reduction technique is recommended.

This approach will therefore be employed in the future for the analysis of dynamic toughness tests performed in upper shelf conditions in the framework of the Tractebel Convention and/or the advanced analysis of Belgian surveillance capsules.

Acknowledgments

My thanks to Jean-Louis Puzzolante for performing the dynamic toughness tests and to Rachid Chaouadi and Marc Scibetta for several interesting and fruitful discussions.

References

[1] K. Wallin, *Effect of Strain Rate on the Fracture Toughness Reference Temperature T_o for Ferritic Steels*, in "Recent Advances in Fracture", R.K. Mahidhara, et al. Eds., The Minerals, Metals & Materials Society, 1997.

[2] E. Lucon and R. Chaoaudi, *Radiation Damage Assessment by the Use of Dynamic Toughness Measurements on Pre-Cracked Charpy Specimens*, in "Effects of Radiation on Materials: 20th International Symposium", ASTM STP 1405, S.T. Rosinski, M.L. Grossbeck, T.R. Allen and A.S. Kumar, Eds., ASTM, 2001, pp.68-78.

[3] J.B. Hall, and K.K.Yoon, *Quasi-static Loading Rate Effect on the Master Curve Reference Temperature of Ferritic Steels and Implications*, Proceedings of the 2003 ASME Pressure Vessels and Piping Conference, July 28-31, 2003, Cleveland.

[4] ESIS Technical Committee 5, *Proposed Standard Methods for Instrumented Pre-cracked Charpy Impact Testing of Steels*, Draft 19: April 2005.

[5] E. Lucon, M. Scibetta and R. Chaouadi, *Applicability of the Master Curve Approach to a RPVS with Various Types of Cleavage Initiators: 20MnMoNi55*, SCK•CEN Report R-3398, February 2000 (restricted).

[6] R. Chaouadi, M. Scibetta and K. Onizawa, *On the Use of the Master Curve Concept and Charpy Size Specimen to Characterize Fracture Toughness in the Transition Regime – Part II: RPV Steel with Low Upper Shelf – A533B Cl.1 (JSPS)*, SCK•CEN Report R-3326, March 1999 (restricted).

[7] K. Wallin and A. Laukkanen, *Improved Crack Growth Corrections for J–R-curve Testing*, Engineering Fracture Mechanics, Vol. 71, Issue 11, July 2004, pp. 1601-1614.

[8] C.S.N.I Specialist Meeting on Instrumented Precracked Charpy Testing, EPRI NP-2102-LD, November 1981.

[9] H. Ernst, P.C. Paris, M. Rossow and J.W. Hutchinson, *Analysis of Load-Displacement Relationship to Determine J-R Curve and Tearing Instability Material Properties*, in "Fracture Mechanics", ASTM STP 677, C.W. Smith, Ed., ASTM, 1979, pp. 581-599.

[10] E. Lucon, M. Scibetta and E. van Walle, *Applying the Normalization Technique for Measuring the Upper Shelf Toughness Properties of RPV Steels*, SCK•CEN Report BLG-915, September 2002 (unclassified).

[11] H.J. Schindler, *Estimation of the Dynamic J-R-curve from a Single Impact Bending Test*, Proceedings of the 11th European Conference on Fracture, ECF11, Poitiers (France), 1996, EMAS Publisher, pp.2007-2012.

[12] H.J. Schindler, *Estimation of Fracture Toughness from Charpy Tests – Theoretical Relations*, in "Pendulum Impact Testing: A Century of Progress", ASTM STP 1380, T. Siewert and M.P. Manahan, Sr., Eds., ASTM, West Conshohocken, 1999, pp. 337-353.

[13] R. Chaouadi, *Crack Resistance Determination from the Load-Displacement Test Record*, SCK•CEN Report R-3712, March 2003 (restricted).

[14] R. Chaouadi and A. Fabry, *On the Utilization of the Instrumented Charpy Impact Test for Characterizing the Flow and Fracture Behaviour of Reactor Pressure Vessel Steels*, in "From Charpy to Present Impact Testing", D. François and A. Pineau, Eds., Elsevier Science Ltd and ESIS, 2002, pp. 103-117.

[15] ESIS P2-92, *ESIS Procedure for Determining the Fracture Behaviour of Materials*, January 1992.

[16] T.L. Anderson, "Fracture Mechanics – Fundamentals and Applications", Second Edition, CRC Press, 1995.